

## Article

# A 2D Hyperchaotic Map: Amplitude Control, Coexisting Symmetrical Attractors and Circuit Implementation

Xuejiao Zhou <sup>1</sup>, Chunbiao Li <sup>1,2,3,\*</sup> , Xu Lu <sup>1</sup>, Tengfei Lei <sup>3</sup>  and Yibo Zhao <sup>1</sup>

<sup>1</sup> Jiangsu Collaborative Innovation Center of Atmospheric Environment and Equipment Technology (CICAEET), Nanjing University of Information Science & Technology, Nanjing 210044, China; 20191219076@nuist.edu.cn (X.Z.); 20171305133@nuist.edu.cn (X.L.); ybzhao@nuist.edu.cn (Y.Z.)

<sup>2</sup> School of Artificial Intelligence, Nanjing University of Information Science & Technology, Nanjing 210044, China

<sup>3</sup> Collaborative Innovation Center of Memristive Computing Application (CICMCA), Qilu Institute of Technology, Jinan 250200, China; leitengfei2017@qlit.edu.cn

\* Correspondence: goontry@126.com or chunbiaolee@nuist.edu.cn; Tel.: +86-139-1299-3098

**Abstract:** An absolute value function was introduced for chaos construction, where hyperchaotic oscillation was found with amplitude rescaling. The nonlinear absolute term brings the convenience for amplitude control. Two regimes of amplitude control including total and partial amplitude control are discussed, where the attractor can be rescaled separately by two independent coefficients. Symmetrical pairs of coexisting attractors are captured by corresponding initial conditions. Circuit implementation by the platform STM32 is consistent with the numerical exploration and the theoretical observation. This finding is helpful for promoting discrete map application, where amplitude control is realized in an easy way and coexisting symmetrical sequences with opposite polarity are obtained.

**Keywords:** amplitude control; coexisting symmetric attractors; hyperchaotic map



**Citation:** Zhou, X.; Li, C.; Lu, X.; Lei, T.; Zhao, Y. A 2D Hyperchaotic Map: Amplitude Control, Coexisting Symmetrical Attractors and Circuit Implementation. *Symmetry* **2021**, *13*, 1047. <https://doi.org/10.3390/sym13061047>

Academic Editor: Giuseppe Grassi

Received: 26 April 2021

Accepted: 8 June 2021

Published: 10 June 2021

**Publisher's Note:** MDPI stays neutral with regard to jurisdictional claims in published maps and institutional affiliations.



**Copyright:** © 2021 by the authors. Licensee MDPI, Basel, Switzerland. This article is an open access article distributed under the terms and conditions of the Creative Commons Attribution (CC BY) license (<https://creativecommons.org/licenses/by/4.0/>).

## 1. Introduction

Chaos has been widely used in image encryption [1–6] and secure communication [7–9]. Adjusting the amplitude of chaos without damaging its engineering application is an important issue because of the butterfly effect. However, there is still much work to do for the rescaling of broadband chaotic sequences. Difficulty modulation with broadband chaotic signal, amplitude [10–13], symmetry [14–17], and multistability [18–21] have been extensively studied in a nonlinear field. In practical engineering applications, linear transformations are usually necessary but sometimes are unpermitted to obtain the required geometric scale in designed hardware. The difficulty hidden in circuit design and debugging increases the value of amplitude control in chaos.

The non-bifurcation parameter is usually applied in the dynamical system to rescale the signal amplitude without changing the Lyapunov exponents, which is significant for the application of chaos. Appropriate signal control can save the modulator in chaos-based applications, including amplitude control [22–24] and offset control [25–28]. In continuous systems, amplitude control with independent control knobs and coexisting symmetric attractors have been widely studied, but in discrete mapping the amplitude control with a single parameter has not received enough attention. For example [29–32], the multistable phenomenon of the map has been discussed in detail, and the position of the phase trajectory through the multistability to achieve the purpose of amplitude control was given, but this ignored a method of directly adjusting the signal amplitude with a single knob. Besides, in many discrete maps like [33], although there are abundant attractor coexistence phenomena, there are no symmetrical coexisting attractors.

In this paper, a two-dimensional hyperchaotic map was given with two independent amplitude knobs, and the map also had a pair of symmetrical coexisting attractors in some

cases. The amplitude control characteristics of the map and the symmetry of the coexisting attractors are analyzed. In Section 2, the hyperchaotic mapping model is constructed and the basic chaotic dynamics behavior is analyzed. In Section 3, the realization method of amplitude control is discussed. The symmetry of the coexisting attractors is discussed in Section 4. In Section 5, the map is implemented through a digital platform. Finally, we give the conclusions and discussion.

## 2. A New 2D Hyperchaotic Map and Its Dynamic Analysis

### 2.1. Model and Its Fixed Points Analysis

Absolute value function is often applied to realize chaos in continuous systems [34,35], and here adding absolute value function into discrete mapping as follows

$$\begin{cases} x_{n+1} = ax_n + bx_n|y_n| \\ y_{n+1} = cx_n - 1.25y_n \end{cases} \quad (1)$$

where  $x_n, y_n$  ( $n = 1, 2, 3, \dots$ ) are system state variables;  $a, b, c$ , are system parameters, and none of them is zero.

The stability of the above discrete mapping (1) can be analyzed by means of fixed points. The fixed points of discrete mapping are the elements that map to itself in its domain. The fixed points  $S^* = (x^*, y^*)$  of the two-dimensional mapping (1) can be solved by the following Equation (2)

$$\begin{cases} x^* = ax^* + bx^*|y^*| \\ y^* = cx^* - 1.25y^* \end{cases} \quad (2)$$

By solving Equation (2), we can get  $|y^*| = \frac{1-a}{b} \rightarrow b(1-a) > 0$ .

The Jacobian matrix of map (1) is

$$J = \begin{bmatrix} 1 & bx^* \operatorname{sgn}(y^*) \\ c & -1.25 \end{bmatrix} \quad (3)$$

Substitute the fixed points  $S^* = (x^*, y^*) = (2.25y^*/c, y^*)$  into Equation (3)

$$J^* = \begin{bmatrix} 1 & \frac{2.25by^* \operatorname{sgn}(y^*)}{c} \\ c & -1.25 \end{bmatrix} \quad (4)$$

The map characteristic equation corresponds to the matrix  $J$  written as follows

$$P(\lambda) = (\lambda + 1.25)(\lambda - 1) - 2.25(1 - a) \quad (5)$$

$\lambda_{1,2}$  are the two eigenvalues of Equation (5). When  $P(\lambda) = 0$ , we can get  $\Delta = 14.0625 - 9a$ . Then  $\lambda_{1,2} = \frac{-0.25 \pm \sqrt{\Delta}}{2}$ . When  $-1 < \lambda_{1,2} = \frac{-0.25 \pm \sqrt{\Delta}}{2} < 1$ , we can get  $1 < a < 11/9$ . Therefore, if  $a < 1, b > 0$  or  $a > 11/9, b < 0$  the map has unstable fixed points, and if  $1 < a < 11/9, b < 0$ , the map has stable fixed points.

When  $a = 2.35, b = -1, c = -1$ , IC = (0.1, 0.1) in map (1), the time series of variables  $x, y$  are shown in Figure 1a,b and the phase trajectory is shown in Figure 1c.

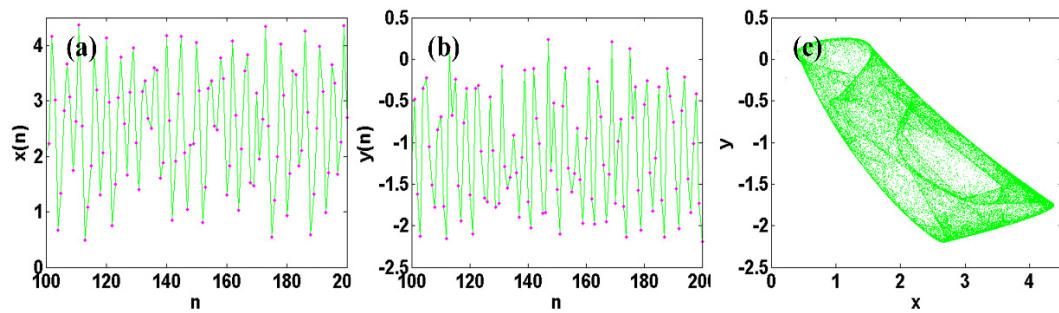


**Figure 1.** The sequence and phase trajectory of map (1) with  $a = 2.35$ ,  $b = -1$ ,  $c = -1$ ,  $IC = (0.1, 0.1)$ : (a)  $x(n)$  sequence, (b)  $y(n)$  sequence, and (c) the phase trajectory.

## 2.2. Bifurcation Analysis

To analyze the nonlinear characteristics of map (1), we set  $b = -1$  and  $c = -1$  and let initial condition  $IC = (0.1, 0.1)$ , the Lyapunov exponent spectra and bifurcation diagram for the region of  $a$  in  $(-2, 2.4)$  are shown in Figure 2. When the parameter  $a$  varies in  $(2, 2.4)$ , it can be seen that when  $a \in (2, 2.15)$ ,  $LE1 = 0$ ,  $LE2 < 0$ , the map is in a quasi-periodical state, and its typical coexisting phase trajectories are shown in Figure 3a. When  $a \in (2.2, 2.234)$ , both exponents are negative, the map is in a periodic state, and its typical coexisting phase trajectories are shown in Figure 3b; when  $a \in (2.247, 2.255)$ ,  $(2.257, 2.32)$ ,  $(2.3256, 2.3259)$ ,  $LE1 > 0$ ,  $LE2 < 0$ , the map is chaotic, and its typical coexisting phase trajectories are shown in Figure 3c–e; when  $a \in (2.283, 2.4)$ , both Lyapunov exponents are greater than zero, therefore the map is hyperchaotic, and its typical coexisting phase trajectories are shown in Figure 3f. The corresponding Lyapunov exponents under different parameters are shown in Table 1.

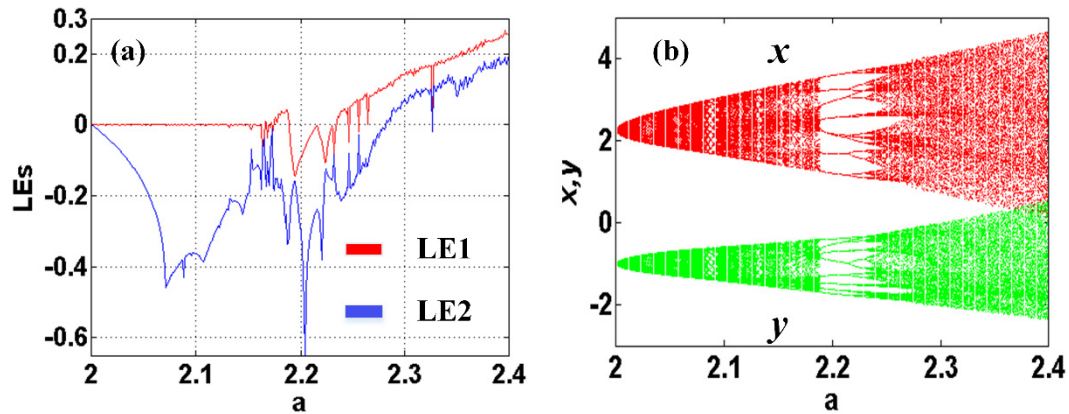


**Figure 2.** Dynamical behavior of map (1) with  $b = -1$ ,  $c = -1$  and initial conditions  $IC = (0.1, 0.1)$ : (a) Lyapunov exponents, (b) bifurcation diagram.

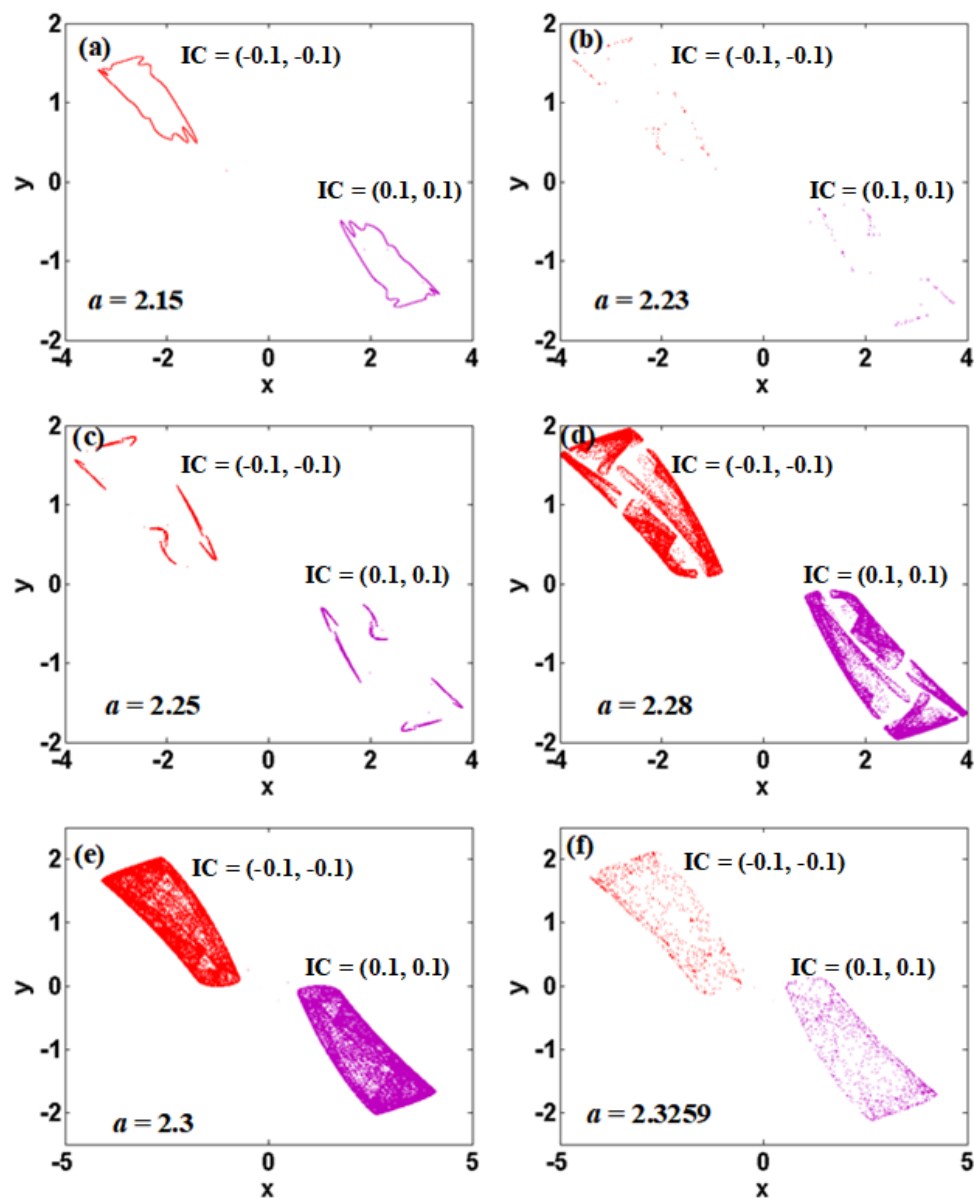


**Figure 3.** Symmetrical coexisting attractors of map (1) with  $b = -1$ ,  $c = -1$  when (a)  $a = 2.15$ , (b)  $a = 2.23$ , (c)  $a = 2.25$ , (d)  $a = 2.28$ , (e)  $a = 2.3$ , (f)  $a = 2.3259$ .

**Table 1.** Phase trajectory types and Lyapunov exponents of map (1) when  $b = -1$ ,  $c = -1$ ,  $IC = (-0.1, -0.1)$ .

$a$	Phase Trajectory Type	LEs
$a = 2.15$	quasi-period	(0, -0.1914)
$a = 2.23$	period	(-0.002709, -0.1558)
$a = 2.25$	chaos	(0.05989, -0.1648)
$a = 2.28$	chaos	(0.1041, -0.01998)
$a = 2.3$	hyperchaos	(0.1403, 0.07291)
$a = 2.3259$	chaos	(0.04464, -0.02)

### 3. Amplitude Control

#### 3.1. Total Amplitude Control

The parameter  $b$  in the map (1) is a single non-bifurcation knob used for total amplitude control [21]. Let  $u_{n+1} = x_{n+1}/b, v_{n+1} = y_{n+1}/b$ , map (1) is changed as follows

$$\begin{cases} u_{n+1} = au_n + b^2u_n|v_n| \\ v_{n+1} = cu_n - 1.25v_n \end{cases} \quad (6)$$

When  $b = 1$ , Equation (6) is equivalent to Equation (1), which indicates that the parameter  $b$  of Equation (1) rescales the amplitude of  $x$  and  $y$  according to  $1/b$ ; that is,  $b$  is the total amplitude parameter.

Therefore, the output sequences are controlled by the non-bifurcation parameter  $b$ . As shown in Figure 4, the amplitude of  $x, y$  are rescaled by the non-bifurcation parameter  $b$ . When  $b = -1$ , the amplitudes of  $x$  and  $y$  are very large; and with the change of  $b$ , it decreases inversely proportional to the absolute value of  $b$ . Figure 4c shows the phase trajectory when the control parameter  $b$  changes.

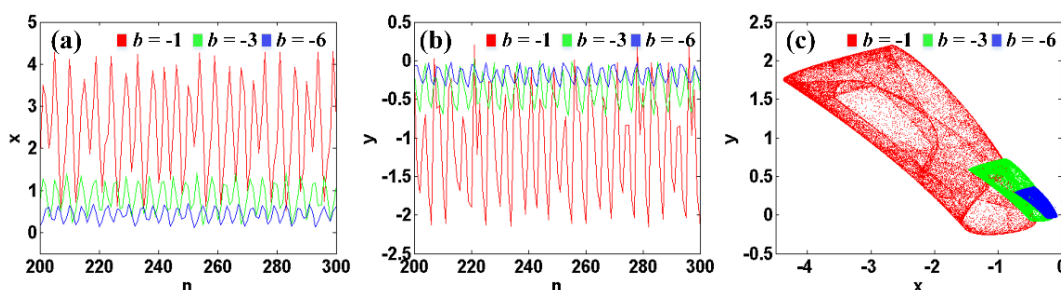


**Figure 4.** Signals and phase trajectories of map (1) with  $a = 2.35, c = -1, IC = (-0.1, -0.1)$  under different rescaling parameter  $b$ : (a)  $x(n)$ , (b)  $y(n)$ , and (c) phase trajectory.

It can be seen from Figure 5 that when the parameter  $b$  changes in the range of  $(-10, 0)$ , the average value of the absolute values of  $x, y$  decreases accordingly in inverse proportion to the absolute value of  $b$ . The Lyapunov exponents spectrum corresponding to the parameter  $b$  in  $(-10, 0)$  remain constant as shown in Figure 5a. It further proves that  $b$  of map (1) only rescales the amplitude of  $x$  without changing the frequency.

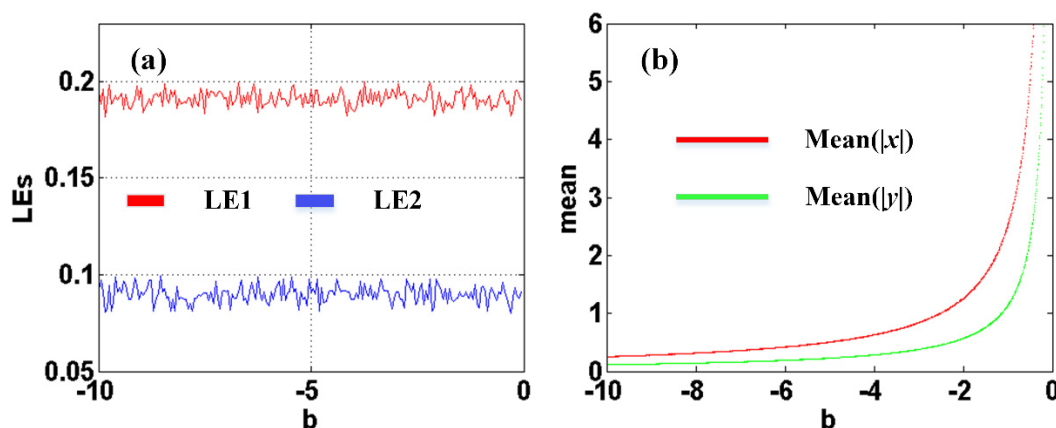


**Figure 5.** Dynamical behavior of map (1) with  $a = 2.35, c = -1, IC = (-0.1, -0.1)$  when  $b$  varies in  $[-10, 0]$ : (a) Lyapunov exponents, (b) average variables of  $|x|$  and  $|y|$ .

### 3.2. Partial Amplitude Control

In map (1), the parameter  $c$  is a single parameter used for partial amplitude control [15]. Here, let  $u_{n+1} = x_{n+1}/c$ ,  $v_{n+1} = y_{n+1}$

$$\begin{cases} u_{n+1} = au_n + bu_n|v_n| \\ v_{n+1} = c^2u_n - 1.25v_n \end{cases} \quad (7)$$

When  $c=1$ , Equation (7) is equivalent to Equation (1), which shows that the parameter  $c$  rescales the amplitude of  $x$  according to  $1/c$ , that is,  $c$  is the partial amplitude parameter.

Therefore, the amplitude of output signal  $x$  is controlled by the parameter  $c$  of map (1). As shown in Figure 6, the amplitude of the signal  $x$  is rescaled by  $c$ . When  $c = -1$ , the amplitude of the  $x$  signal is very large, and as  $c$  changes, it decreases in inverse proportion to the absolute value of  $c$ . Figure 6b shows the phase trajectories when the control parameter  $c$  changes.

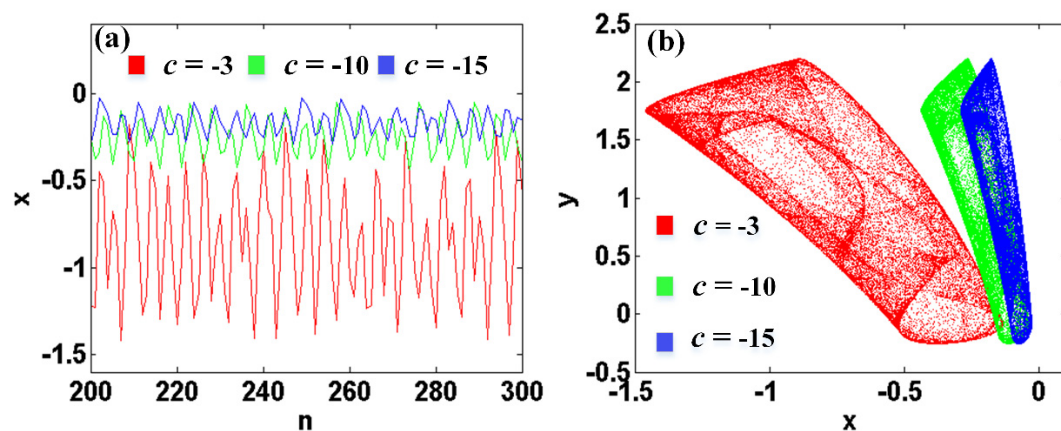


**Figure 6.** Feature of amplitude control in map (1) with  $a = 2.35$ ,  $b = -1$  and IC =  $(-0.1, -0.1)$  for the scaling variable  $c$ : (a)  $x$  signal waveform (b) phase trajectories.

It can also be seen from Figure 7b that when the parameter  $c$  changes within the range of  $(-15, 0)$ , the average value of the absolute value of the state variables  $x$  decreases accordingly in inverse proportion to the absolute value of  $c$ . The Lyapunov exponents spectrum corresponding to parameter  $c$  is shown in Figure 7a, showing that the parameter  $c$  of map (1) only rescales the amplitude of the state variable  $x$  without adjusting the frequency of it.

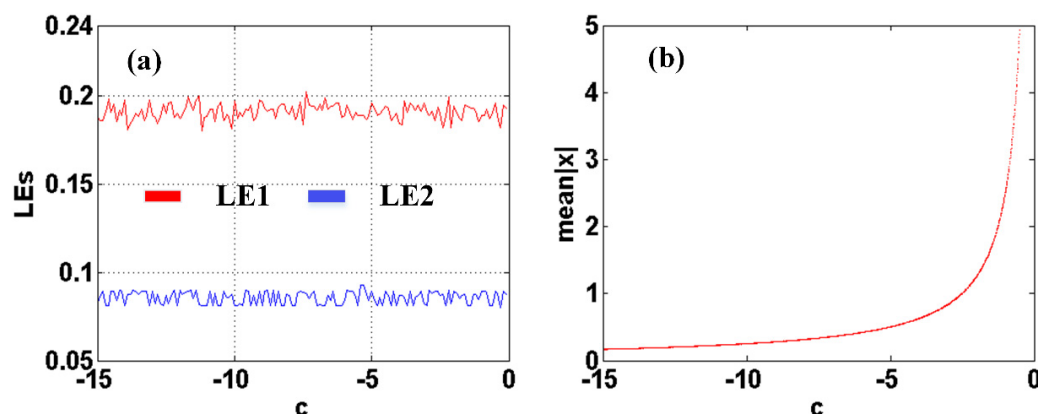


**Figure 7.** Dynamical behavior of map (1) with  $a = 2.35$ ,  $b = -1$  and IC =  $(-0.1, -0.1)$ , when  $c$  varies in  $(-15, 0]$ : (a) Lyapunov exponents, (b) average value of the state variable  $x$ .

#### 4. Bistability with Coexisting Symmetrical Attractors

In the following section, we focus on the multistability of the map. Typically, for the special structure of symmetrical maps, there are coexisting attractors in their basins of attraction in the phase space. Map (1) is a symmetric map, which can be proved by the invariance under the transforming  $x \rightarrow -x, y \rightarrow -y$ . At this time, the polarities on both sides of the map equation remain balanced.

Figure 8 shows the basin of attraction of map (1) with  $a = 2.35, b = -1, c = -1$ , which proves its bistability. Here we use the same color to mark the basin of attraction. There are two areas in different colors in the picture, clearly showing the two types of attractors.

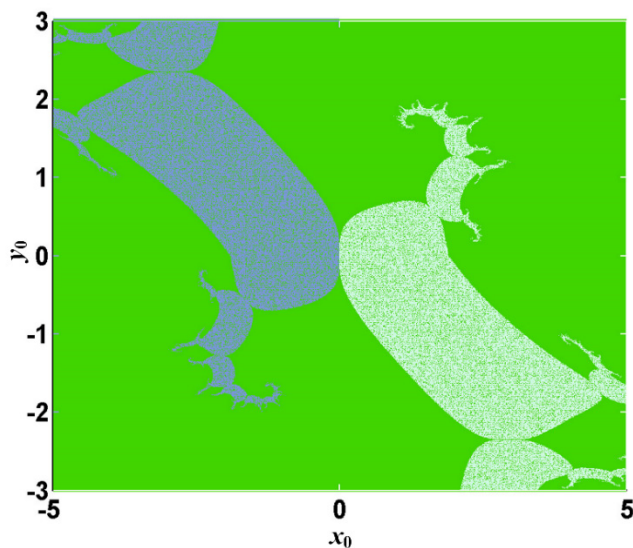


Figure 8. Symmetric basins of attraction for map (1) with  $a = 2.35, b = -1, c = 1$ , Dark turquoise for  $IC = (0.1, 0.1)$ , and Light cyan is for  $IC = (-0.1, -0.1)$ .

The bifurcation of parameter  $b$  for the state variable  $y$  under different initial values is shown in Figure 9, and Figure 10 shows typical phase trajectories of coexisting symmetric attractors. It can also be seen that the parameter  $b$  can modify the symmetric modes of the coexisting attractors under a set of fixed initial conditions. From Figure 10a,b, we can see the parameter  $b$  can freely control the polarity of the sequence of  $y$ .

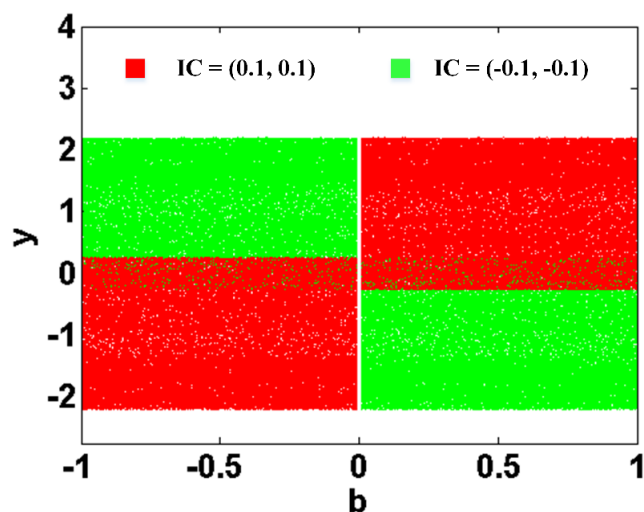


Figure 9. Coexisting bifurcation diagrams of map (1) with different initial conditions and  $a = 2.35, c = -1$ .

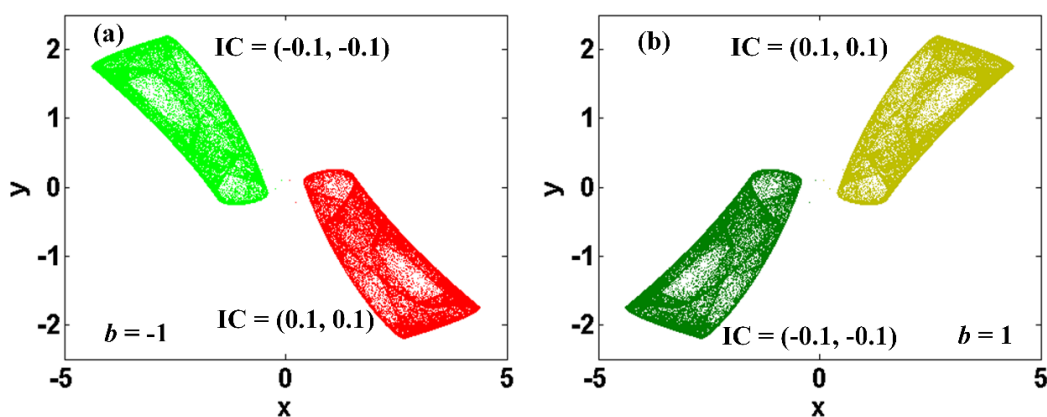


Figure 10. Coexisting symmetric attractors of map (1) with  $a = 2.35, c = -1$ : (a)  $b = -1$ , and (b)  $b = 1$ .

To verify the bistability of map (1), we analyze it in terms of the signal waveforms. Figure 11 shows the signal waveforms of the state variables  $x, y$ . The symmetric attractors are controlled under various parameter  $b$  and  $c$  as shown in Figure 12.

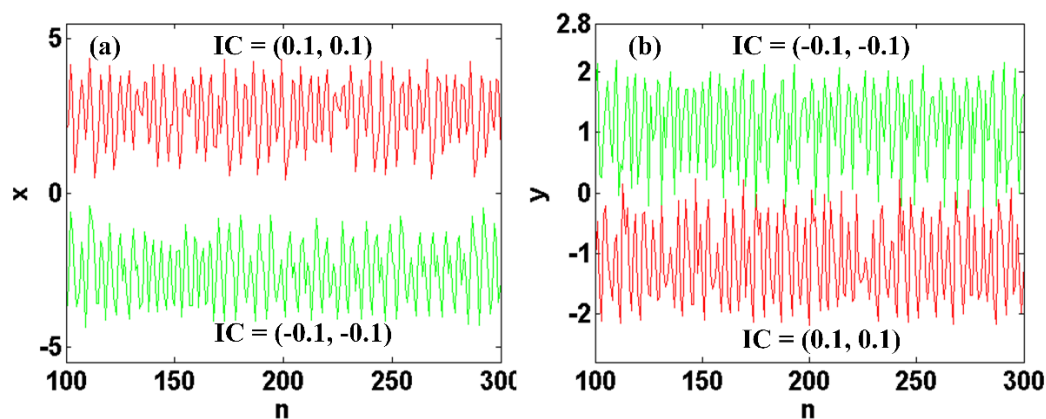


Figure 11. Signal waveforms of map (1) with  $a = 2.35, b = -1, c = -1$ , under various initial values: (a) the state variable  $x$ , (b) the state variable  $y$ .

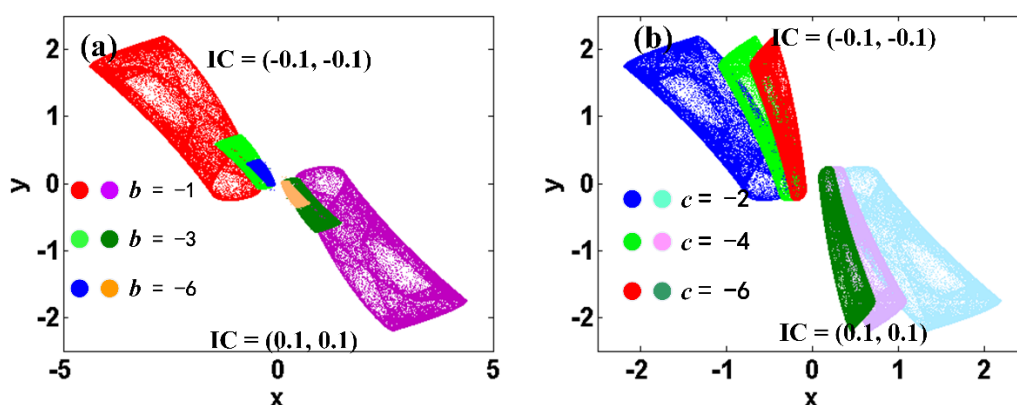


Figure 12. Symmetric attractors of map (1) at different amplitude parameters: (a) total amplitude control with  $c = -1$ , and (b) partial amplitude control with  $b = -1$ .

### 5. Circuit Implementation

In this work, the digital technique is used to demonstrate the dynamic characteristics of map (1). The experimental device mainly includes STM32F103 and 12-bit digital-to-

analog conversion module TLV5618. Two signals of the map (1) are output through two 12-bit digital-to-analog converter (DAC) modules. The experimental circuit platform is shown in Figure 13. Given the corresponding parameter values and initial conditions, the typical phase diagram of the chaotic map can be observed in the oscilloscope, as shown in Figure 14.

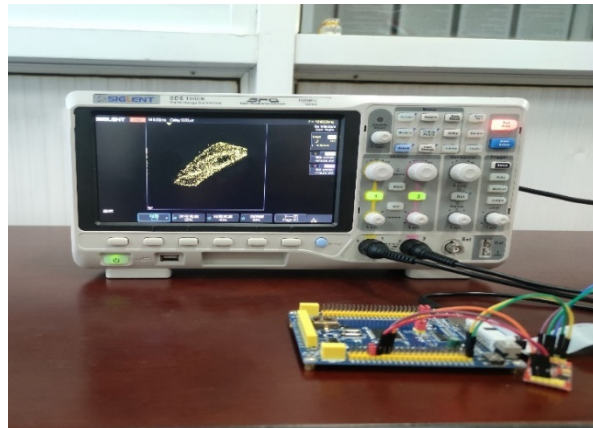


Figure 13. Experimental platform.

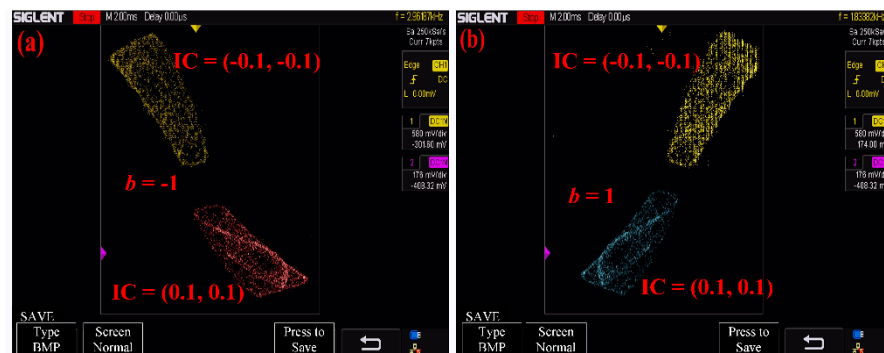


Figure 14. Two modes of the symmetric coexisting attractors in map (1) from the oscilloscope with  $a = 2.35$ ,  $c = -1$ , (a)  $b = -1$ , (b)  $b = 1$ .

## 6. Discussion and Conclusions

In this paper, the dynamical properties of a two-dimensional hyperchaotic map with absolute value function are discussed, and the stability of its fixed points are analyzed in detail. The map can not only realize the global amplitude control by a single controller but can also realize the partial amplitude control by a single knob. These dynamic characteristics are proved by the platform based on STM32F103 chip and the digital-to-analog converter, where the experimental results are in good agreement with the simulation analysis. The special symmetry mode is a new passage for providing coexisting oscillation with inverse polarity of the chaotic signal, which shows great potential in chaos application and deserve further exploration. In future, the simple hyperchaotic map could be applied to the design of random number generators for chaos-based engineering.

**Author Contributions:** Conceptualization, C.L.; methodology, C.L.; software, X.Z.; validation, X.L., T.L. and Y.Z.; formal analysis, X.Z. and X.L.; investigation, Y.Z.; resources, C.L.; data curation, X.Z.; writing—original draft preparation, X.Z.; writing—review and editing, X.Z. and C.L.; visualization, X.Z., T.L. and Y.Z.; supervision, C.L.; project administration, C.L.; funding acquisition, C.L. and X.L. All authors have read and agreed to the published version of the manuscript.

**Funding:** This work was supported financially by the National Natural Science Foundation of China (Grant No. 61871230), the Natural Science Foundation of Jiangsu Province (Grant No. BK20181410) and the Provincial Key Training Programs of Innovation and Entrepreneurship for Undergraduates (Grant No.: 201910300053Z).

**Institutional Review Board Statement:** Not applicable.

**Informed Consent Statement:** Not applicable.

**Data Availability Statement:** The data that support the findings of this study are available from the corresponding author upon reasonable request.

**Conflicts of Interest:** The authors declare no conflict of interest.

## References

1. Yang, F.; Mou, J.; Liu, J.; Ma, C.; Yan, H. Characteristic analysis of the fractional-order hyperchaotic complex system and its image encryption application. *Signal Process.* **2020**, *169*, 107373. [[CrossRef](#)]
2. Peng, G.; Min, F. Multistability analysis, circuit implementations and application in image encryption of a novel memristive chaotic circuit. *Nonlinear Dyn.* **2017**, *90*, 1607–1625. [[CrossRef](#)]
3. Deng, J.; Zhou, M.; Wang, C.; Wang, S.; Xu, C. Image segmentation encryption algorithm with chaotic sequence generation participated by cipher and multi-feedback loops. *Multimed. Tools Appl.* **2021**, 1–20. [[CrossRef](#)]
4. Zeng, J.; Wang, C. A novel hyperchaotic image encryption system based on particle swarm optimization algorithm and cellular automata. *Secur. Commun. Netw.* **2021**, *2021*, 6675565. [[CrossRef](#)]
5. Shah, S.A.; Ahmad, J.; Masood, F.; Shah, S.Y.; Pervaiz, H.; Taylor, W.; Abbasi, Q.H. Privacy-Preserving Wandering Behavior Sensing in Dementia Patients Using Modified Logistic and Dynamic Newton Leipnik Maps. *IEEE Sens. J.* **2021**, *21*, 3669–3679. [[CrossRef](#)]
6. Khan, J.S.; Boulila, W.; Ahmad, J.; Rubaiee, S.; Rehman, A.U.; Alroobaea, R.; Buchanan, W.J. DNA and plaintext dependent chaotic visual selective image encryption. *IEEE Access* **2020**, *8*, 159732–159744. [[CrossRef](#)]
7. Wang, S.; Kuang, J.; Li, J.; Luo, Y.; Lu, H.; Hu, G. Chaos-based secure communications in a large community. *Phys. Rev. E* **2002**, *66*, 065202. [[CrossRef](#)]
8. Kocarev, L.; Halle, K.S.; Eckert, K.; Chua, L.O.; Parlitz, U. Experimental demonstration of secure communications via chaotic synchronization. *Int. J. Bifurc. Chaos* **1992**, *2*, 709–713. [[CrossRef](#)]
9. Li, C.; Liao, X.; Wong, K. Lag synchronization of hyperchaos with application to secure communications. *Chaos Solitons Fractals* **2005**, *23*, 183–193. [[CrossRef](#)]
10. Li, C.; Sprott, J.C. Amplitude control approach for chaotic signals. *Nonlinear Dyn.* **2013**, *73*, 1335–1341. [[CrossRef](#)]
11. Li, C.; Sprott, J.C. Finding coexisting attractors using amplitude control. *Nonlinear Dyn.* **2014**, *78*, 2059–2064. [[CrossRef](#)]
12. Wu, Q.; Hong, Q.; Liu, X.; Wang, X.; Zeng, Z. A novel amplitude control method for constructing nested hidden multi-butterfly and multiscroll chaotic attractors. *Chaos Solitons Fractals* **2020**, *134*, 109727. [[CrossRef](#)]
13. Zang, H.; Gu, Z.; Lei, T.; Li, C.; Jafari, S. Coexisting chaotic attractors in a memristive system and their amplitude control. *Pramana* **2020**, *94*, 1–9. [[CrossRef](#)]
14. Li, C.; Sprott, J.C.; Xing, H. Constructing chaotic systems with conditional symmetry. *Nonlinear Dyn.* **2017**, *87*, 1351–1358. [[CrossRef](#)]
15. Lu, T.; Li, C.; Jafari, S.; Min, F. Controlling coexisting attractors of conditional symmetry. *Int. J. Bifurc. Chaos* **2019**, *29*, 1950207. [[CrossRef](#)]
16. Kengne, L.K.; Kengne, J.; Fotsin, H.B. The effects of symmetry breaking on the dynamics of a simple autonomous jerk circuit. *Analog Integr. Circuits Signal Process.* **2019**, *101*, 489–512. [[CrossRef](#)]
17. Zhang, X.; Li, C.; Lei, T.; Liu, Z.; Tao, C. A symmetric controllable hyperchaotic hidden attractor. *Symmetry* **2020**, *12*, 550. [[CrossRef](#)]
18. Leutcho, G.D.; Kengne, J.; Kengne, L.K. Dynamical analysis of a novel autonomous 4-D hyperjerk circuit with hyperbolic sine nonlinearity: Chaos, antimonotonicity and a plethora of coexisting attractors. *Chaos Solitons Fractals* **2018**, *107*, 67–87. [[CrossRef](#)]
19. Lai, Q.; Chen, C.; Zhao, X.W.; Kengne, J.; Volos, C. Constructing chaotic system with multiple coexisting attractors. *IEEE Access* **2019**, *7*, 24051–24056. [[CrossRef](#)]
20. Bao, H.; Hua, Z.; Wang, N.; Zhu, L.; Chen, M.; Bao, B. Initials-Boosted Coexisting Chaos in a 2-D Sine Map and Its Hardware Implementation. *IEEE Trans. Ind. Inform.* **2020**, *17*, 1132–1140. [[CrossRef](#)]

21. Wang, Z.; Abdolmohammadi, H.R.; Alsaadi, F.E.; Hayat, T.; Pham, V.T. A new oscillator with infinite coexisting asymmetric attractors. *Chaos Solitons Fractals* **2018**, *110*, 252–258. [[CrossRef](#)]
22. Li, C.L.; Li, W.; Zhang, J.; Xie, Y.X.; Zhao, Y.B. Amplitude-Phase Modulation, Topological Horseshoe and Scaling Attractor of a Dynamical System. *Commun. Theor. Phys.* **2016**, *66*, 297. [[CrossRef](#)]
23. Li, C.; Sprott, J.C.; Yuan, Z.; Li, H. Constructing chaotic systems with total amplitude control. *Int. J. Bifurc. Chaos* **2015**, *25*, 1530025. [[CrossRef](#)]
24. Hu, W.; Akgul, A.; Li, C.; Zheng, T.; Li, P. A switchable chaotic oscillator with two amplitude–frequency controllers. *J. Circuits Syst. Comput.* **2017**, *26*, 1750158. [[CrossRef](#)]
25. Li, C.; Wang, X.; Chen, G. Diagnosing multistability by offset boosting. *Nonlinear Dyn.* **2017**, *90*, 1335–1341. [[CrossRef](#)]
26. Zhang, S.; Zeng, Y.; Li, Z.; Zhou, C. Hidden extreme multistability, antimonotonicity and offset boosting control in a novel fractional-order hyperchaotic system without equilibrium. *Int. J. Bifurc. Chaos* **2018**, *28*, 1850167. [[CrossRef](#)]
27. Li, C.; Sun, J.; Lu, T.; Lei, T. Symmetry evolution in chaotic system. *Symmetry* **2020**, *12*, 574. [[CrossRef](#)]
28. Chen, M.; Ren, X.; Wu, H.; Xu, Q.; Bao, B. Interpreting initial offset boosting via reconstitution in integral domain. *Chaos Solitons Fractals* **2020**, *131*, 109544. [[CrossRef](#)]
29. Bao, B.C.; Li, H.Z.; Zhu, L.; Zhang, X.; Chen, M. Initial-switched boosting bifurcations in 2D hyperchaotic map. *Chaos Interdiscip. J. Nonlinear Sci.* **2020**, *30*, 033107. [[CrossRef](#)]
30. Li, H.; Bao, H.; Zhu, L.; Bao, B.; Chen, M. Extreme Multistability in Simple Area-Preserving Map. *IEEE Access* **2020**, *8*, 175972–175980. [[CrossRef](#)]
31. Zhang, L.P.; Liu, Y.; Wei, Z.C.; Jiang, H.B.; Bi, Q.S. A novel class of two-dimensional chaotic maps with infinitely many coexisting attractors. *Chin. Phys. B* **2020**, *29*, 060501. [[CrossRef](#)]
32. Yan, B.; He, S.; Sun, K.; Wang, S. Complexity and Multistability in the Centrifugal Flywheel Governor System with Stochastic Noise. *IEEE Access* **2020**, *8*, 30092–30103. [[CrossRef](#)]
33. Hua, Z.; Zhou, B.; Zhou, Y. Sine-transform-based chaotic system with FPGA implementation. *IEEE Trans. Ind. Electron.* **2017**, *65*, 2557–2566. [[CrossRef](#)]
34. Zhang, X.; Li, C.; Min, F.; Iu, H.H.C.; Gao, H. Broken Symmetry in a Memristive Chaotic Oscillator. *IEEE Access* **2020**, *8*, 69222–69229. [[CrossRef](#)]
35. Zhang, X.; Li, C.; Chen, Y.; Herbert, H.C.; Lei, T. A memristive chaotic oscillator with controllable amplitude and frequency. *Chaos Solitons Fractals* **2020**, *139*, 110000. [[CrossRef](#)]